AD-A072 851 RDP INC WALTHAM MASS F/G 9/2
ATMOSPHERE EXPLORER MESA ACCELEROMETER DENSITY DATA BASE.(U)
JUN 78 R W FIORETTI, L D COX F19628-76-C-0169
UNCLASSIFIED AFGL-TR-79-0062 NL

| OF |
AD
A072851

END
DATE
FILMED
9-79
DDC

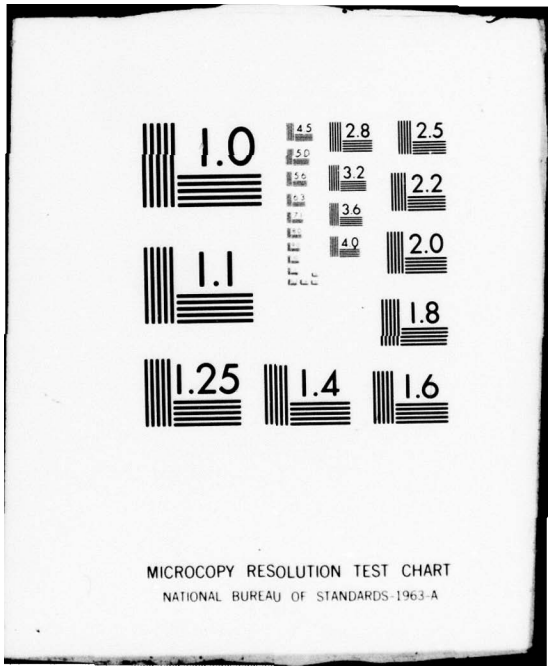
1.0
1.1
1.25
1.4
1.6
1.8
2.0
2.2
2.5
2.8
3.2
3.6
4.0
4.5
5.0
5.6
6.3
MICROCOPY RESOLUTION TEST CHART
NATIONAL BUREAU OF STANDARDS-1963-A

AFGL-TR-79-0062

ATMOSPHERE EXPLORER MESA ACCELEROMETER DENSITY DATA BASE

Robert W. Fioretti
Lawrence D. Cox

RDP, Inc.
391 Totten Pond Road
Waltham, Massachusetts 02154

FINAL REPORT

16 March 1976 - 14 June 1978

15 June 1978

Approved for public release, distribution unlimited.

Prepared for:

AIR FORCE GEOPHYSICS LABORATORY
AIR FORCE SYSTEMS COMMAND
UNITED STATES AIR FORCE
HANSCOM AFB, MASSACHUSETTS 01731

UNCLASSIFIED

SECURITY CLASSIFICATION OF THIS PAGE (When Data Entered)

REPORT DOCUMENTATION PAGE	READ INSTRUCTIONS BEFORE COMPLETING FORM
1. REPORT NUMBER: AFGL-TR-79-0062	2. GOVT ACCESSION NO.
	3. RECIPIENT'S CATALOG NUMBER: Final rept.
4. TITLE (and Subtitle): ATMOSPHERE EXPLORER MESA ACCELEROMETER DENSITY DATA BASE,	5. TYPE OF REPORT & PERIOD COVERED: 16 Mar 76 — 14 June 78
	6. PERFORMING ORG. REPORT NUMBER: FINAL REPORT
7. AUTHOR(s): ROBERT W. FIORETTI, LAWRENCE D. COX	8. CONTRACT OR GRANT NUMBER(s): F19628-76-C-0169
9. PERFORMING ORGANIZATION NAME AND ADDRESS: RDP, Inc. 391 Totten Pond Road Waltham, Ma. 02154	10. PROGRAM ELEMENT, PROJECT, TASK AREA & WORK UNIT NUMBERS: 62101F 6690 02AL
11. CONTROLLING OFFICE NAME AND ADDRESS: Air Force Geophysics Laboratory Hanscom AFB, MA 01731 Monitor/Frank Marcos/LKB	12. REPORT DATE: 15 June 1978
	13. NUMBER OF PAGES: 34
14. MONITORING AGENCY NAME & ADDRESS (if different from Controlling Office): 35 p.	15. SECURITY CLASS. (of this report): UNCLASSIFIED
	15a. DECLASSIFICATION/DOWNGRADING SCHEDULE

16. DISTRIBUTION STATEMENT (of this Report)

Approved for public release; distribution unlimited.

17. DISTRIBUTION STATEMENT (of the abstract entered in Block 20, if different from Report)

18. SUPPLEMENTARY NOTES

19. KEY WORDS (Continue on reverse side if necessary and identify by block number)

Data processing, Atmosphere Explorer, MESA Accelerometer, Satellite, Data Base.

20. ABSTRACT (Continue on reverse side if necessary and identify by block number)

This report describes the development of an extensive neutral atmospheric density data base generated from MESA accelerometer experiments. This data base represents the most extensive set of neutral density measurements in existence. Studies by AFGL scientists utilizing this data base are in preparation.

DD FORM 1 JAN 73 1473 EDITION OF 1 NOV 65 IS OBSOLETE

UNCLASSIFIED

SECURITY CLASSIFICATION OF THIS PAGE (When Data Entered)

409955

FOREWORD

The efforts described herein were performed under contract to the Atmospheric Structure Branch (LKB), Aeronomy Division of the Air Force Geophysics Laboratory (AFGL), Hanscom Air Force Base, Bedford, Massachusetts.

Table of Contents

List of Illustrations

List of Illustrations (Cont.)

1. INTRODUCTION

The efforts described herein are part of a project to develop and implement a data processing software system for the management and analysis of data received from the AFGL MESA (Miniature Electrostatic Accelerometer) experiment flown aboard three of the NASA Atmosphere Explorer (AE) series of satellites, AE-C, AE-D, and AE-E. The MESA data processing system and the analytical techniques utilized to extract drag accelerations from the total accelerometer output signal of each of these satellites have been described previously (1, 2).

This report describes the development of an extensive neutral atmospheric density data base generated from the MESA experiments on these satellites (taken from the elliptical phases of their respective missions). This data base represents the most extensive set of neutral density measurements in existence. Knowledge of atmospheric density and its variations is required for satisfactory low altitude satellite design, operation and orbit prediction.

Also included in this report is a description of an empirical model of density given as a function of altitude, latitude, and geomagnetic activity which was generated from this data base. Further such studies by AFGL scientists utilizing this data base are in preparation.

1.1 Satellite Characteristics

The Atmosphere Explorer program involved three low-altitude satellites designed to permit a coordinated study of the thermosphere. A detailed description of the AE satellites and their mission may be found in Reference (3).

AE-C, AE-D, and AE-E were launched into low perigee-high eccentricity orbits. The on-board propulsion system was used to maintain an elliptical orbit for approximately one year for AE-C and AE-E. AE-D data acquisitions were terminated after three and one-half months when the spacecraft power system failed. AE-C and AE-E were put into

circular orbits near 250 km following their elliptical orbit phases. Data were acquired in both spinning (4 rpm) and despun (1 rpo) modes.

The AE data base as presently configured and stored at AFGL includes only elliptical orbit data. Circular orbit data are stored at the AE computer facility at NASA/GSFC.

1.2 MESA Experiment

The accelerometer experiment on the AE satellites provides extremely accurate measurements of orbital accelerations. Three single-axis instruments orthogonally mounted were flown on each AE satellite. Two sensors were placed with their sensitive axes in the spacecraft XY plane. These two instruments were used to provide redundant capability for density measurement, particularly during the despun mode, as well as to monitor the orbit-adjust propulsion system. The third sensor was placed with its sensitive axis along the spacecraft Z-axis. This sensor was used to monitor spacecraft roll and horizontal winds, particularly in the despun mode of operation. A complete description of the MESA experiment may be found in Reference (3).

The approach taken to extract drag accelerations from the total accelerometer signal was provided by numerical filtering techniques. For despun orbits atmospheric drag information are sensed as low frequency accelerations whose amplitudes vary between 10^{-8} and 5×10^{-4} g's depending upon satellite altitude. To measure the drag information a low pass filter was used. For spinning orbits the drag information appears as a modulated signal at the spin frequency. A band-pass filter was designed to process these data. A complete description of the filtering techniques may be found in Reference (2).

1.3 Data Base Development

The MESA Data Reduction System (DRS) which has been developed and previously described in Reference (1) is capable of extracting raw telemetry data from the AE data base, editing and temperature-correcting

the telemetry data, extracting atmospheric drag values utilizing digital filtering techniques, and calculating atmospheric density information. These density data (calculated every quarter-second) along with particular orbital and attitude information, are stored in MESA geophysical unit (GU) files. In addition, density values are interpolated from these GU files and stored in 15-second intervals in unified abstract (UA) history files for use by other experimenters.

The MESA density data base was developed from the UA history files in the following manner. For each satellite (AE-C, D and E), orbital and density values were calculated at 5-km intervals from 135 km to 245 km, utilizing Lagrangian interpolation techniques and were stored in data files on the AE computer. The data from these files were then shipped to AFGL for use on the AFGL CDC 6600 computers.

At AFGL the data were then merged with Jacchia 71 and MSIS model density values, solar flux, magnetic index Kp, and geomagnetic latitude and longitude values. These parameters make up the MESA density data base for each AE satellite.

In analyzing the data from these data bases it became evident that a time history data base would also be very useful. We, therefore, reordered the altitude data base in chronological format for each satellite. This resulted in a time history of density values given in 5-km intervals for each orbit of processed data.

Having distinct data bases for each satellite (-C, -D, -E), we next combined data from all three satellites and generated a composite data base. This was done for both the altitude and time history data bases, and these two composite data bases make up the present AE data base. The format of the AE data base tapes is given in Figure 1.

1.4 S3-1 Data Base

S3-1 satellite orbital parameters and accelerometer density values were provided to us in approximately 6-second increments for each orbit processed. From these data orbital and density values were

Data Base Tape Format
Altitude Files

The data base is stored by satellite and altitude in 5-km intervals. Each tape contains many files, each file contains two types of records – header and data records. The tapes are blocked, binary, 800 BPI.

1. Header Record

The first record of each (altitude) file is a header record in the following format:

Word	Description	Format
0.1	word count (IWD=40)	I
0.2	group count (JGP=1)	I
1	satellite ID (AE-? or S3-1)	A
2	experimental name ('MESA')	A
3	satellite altitude - km	I
4	Run date (YYDDD)	I
5	#files*100 + file#	I
6-40	blank	R

2. Data Records

The remaining records of each file are data records in the following format:

Word	Description	Format
0.1	word count (IWD=40)	I
0.2	group count (JGP=12)	I
1	orbit number	I
2	date - YYDDD	I
3	GMT - total seconds	I
4	GMT - hours	I
5	GMT - minutes	I
6	GMT - sec.	I
7	local time - hours	I
8	local time - minutes	I
9	local time - sec	I
10	LEG (U=upleg, D=downleg)	A
11	day/night (D=day, N=night)	A
12	Spin/despun (S=spin, D=despun)	A
13	geographic latitude	F
14	geographic longitude (+E)	I
15	geomagnetic latitude	F

Figure 1. Data Base File Format

Word	Description	Format
16	geomagnetic longitude (+E)	I
17	invariant latitude	F
18	density - gm/cc	F
19	J71 model density	F
20	J71 model density (Kp = 2)	F
21	MSIS model density	F
22	ratio (measured/J71)	F
23	ratio (measured/J71 (Kp = 2))	F
24	ratio (measured/MSIS)	F
25	Ap - daily	F
26	Ap (6.7 hr. lag)	I
27	Kp (6.7 hr. lag)	F
28	F7 (day lag)	F
29	FB7 (81 day average)	F
30	blank	F
31	Kp - 0 hour lag	F
32	Kp - 3 hour lag	F
33	Kp - 6 hour lag	F
34	Kp - 9 hour lag	F
35	Kp - 12 hour lag	F
36	average value of 32-35 above	F
37-40	blank	F

3. An EOF follows the last data record.

Figure 1. Data Base File Format (Cont.)

calculated at 5 km intervals from 150 km to 250 km utilizing Lagrangian interpolation techniques and were stored in data files on the AFGL computer. As with the AE data base, the S3-1 data were merged with J71 and MSIS model values, solar flux, magnetic index Kp and geomagnetic latitude and longitude values. This merged data file comprised the S3-1 data base.

The S3-1 data base information was further merged with the composite AE data base. This was done for both the altitude and time history files, and those two new composite data bases make up the present AE/S3 accelerometer density data base.

2. DATA BASE PROPERTIES [1]

As mentioned previously the present density data base includes only elliptical orbit data. Table 1 provides orbital characteristics and dates of elliptical orbit data acquisition for each satellite. The altitudes at which data were obtained are shown (shaded areas) in Figure 2.

Table 1. Satellite Orbital Characteristics and Data Acquisition Periods

Satellite	Launch	End Elliptical Data Acquisition	Inclination	Initial Perigee	Initial Apogee
AE-C	Dec 73	Nov 74	68°	156 km	4000 km
S3-1	Oct 74	May 75	97°	160 km	4000 km
AE-D	Oct 75	Jan 76	90°	156 km	3800 km
AE-E	Nov 75	Nov 76	20°	157 km	3000 km

2.1 Statistical Properties

Density values calculated at 5-km intervals were stored in the data base. Associated with each point is the corresponding J71 and MSIS model value, ephemeris data, solar flux, and K_p value. A histogram of the data distribution as a function of geographic latitude for each satellite

[1] Portions of this section were taken directly from Reference (4).

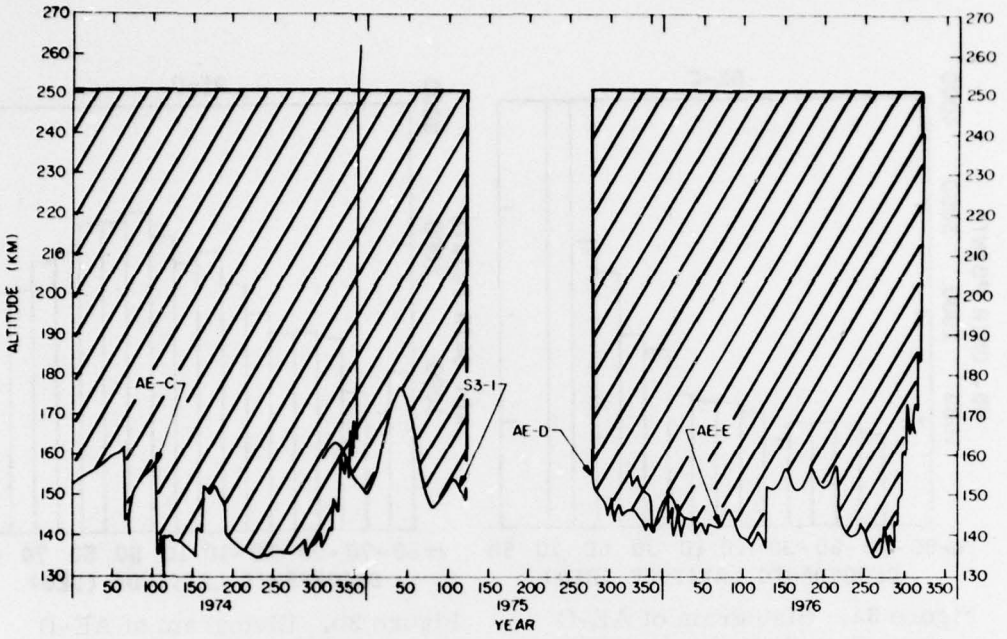

Figure 2. Distribution of Density Data

is given in Figures 3a through 3d. These figures show the number of data points obtained in each 10° latitude band. The percentages of the total amount of data (combining the four sets) in the latitude bands $0 \pm 20°$, $|20 - 50°|$ $|50 - 70°|$, and $|70 - 90°|$ are 47%, 25%, 18%, and 11%, respectively. The large amount of near equatorial data is due to the low inclination of AE-E and the precession of perigee for the other satellites as indicated by Figure 2. The data above $|70°|$ are provided by AE-D and S3-1. Although relatively small in percentage of total data, 12,822 points were obtained at these latitudes. Figures 4a through 4d show the data distribution as a function of local time, given the number of points within each one hour interval. The figures show excellent local time coverage provided by AE-C and -E. The distribution of data with respect to geomagnetic activity is shown in Figures 5a through 5d. These plots give the number of measurements during which the three-hourly K_p index (with a six hour lag) fell within specific one unit intervals. Approximately 20% of all the data occur during conditions when the average K_p

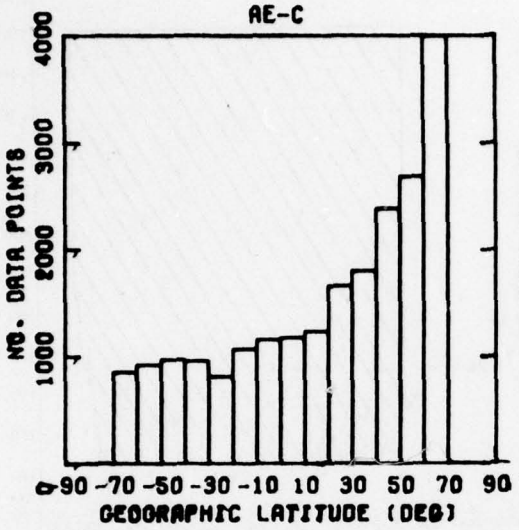

Figure 3a. Histogram of AE-C Data Distribution as a Function of Geographic Latitude

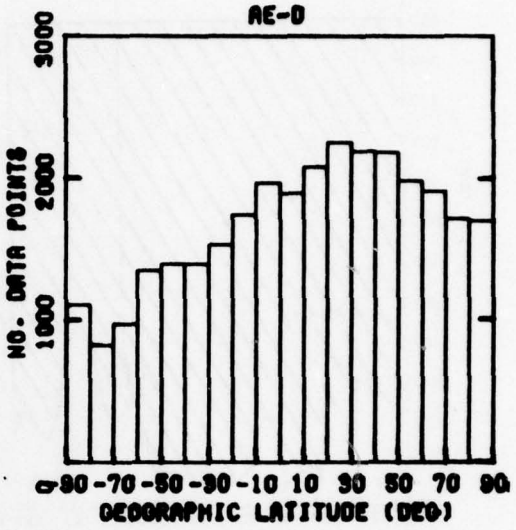

Figure 3b. Histogram of AE-D Data Distribution as a Function of Geographic Latitude

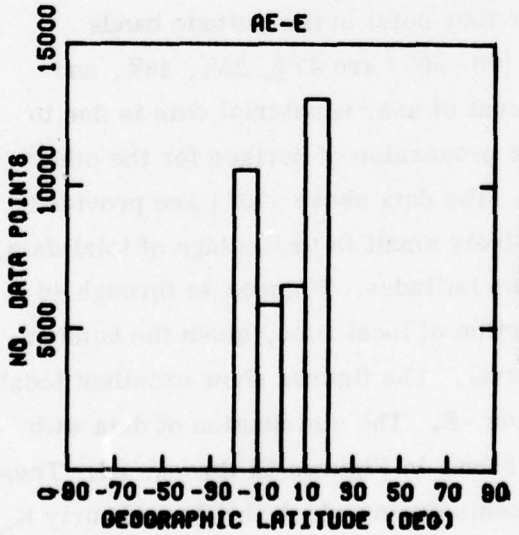

Figure 3c. Histogram of AE-E Data Distribution as a Function of Geographic Latitude

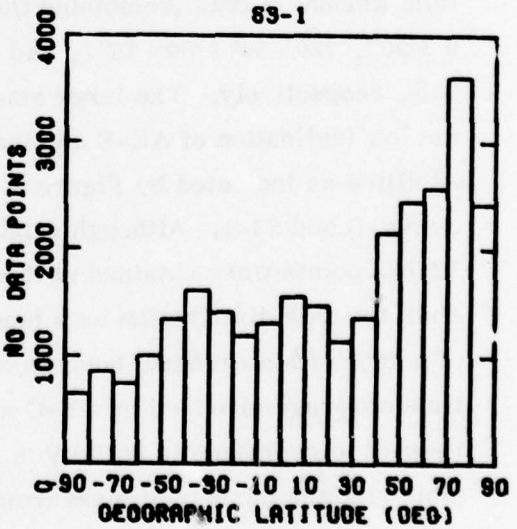

Figure 3d. Histogram of S3-1 Data Distribution as a Function of Geographic Latitude

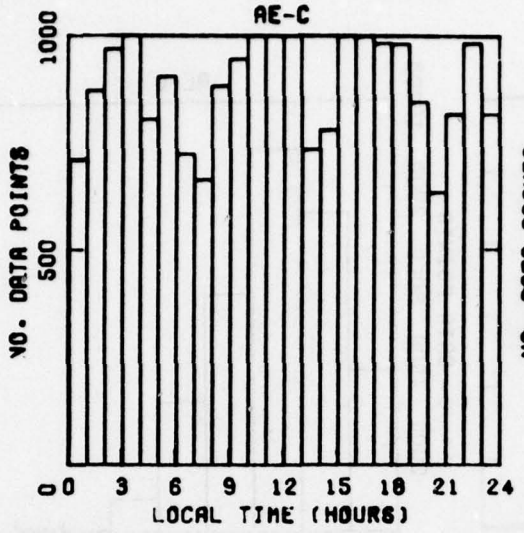

Figure 4a. Histogram of AE-C Data Distribution as a Function of Local Time

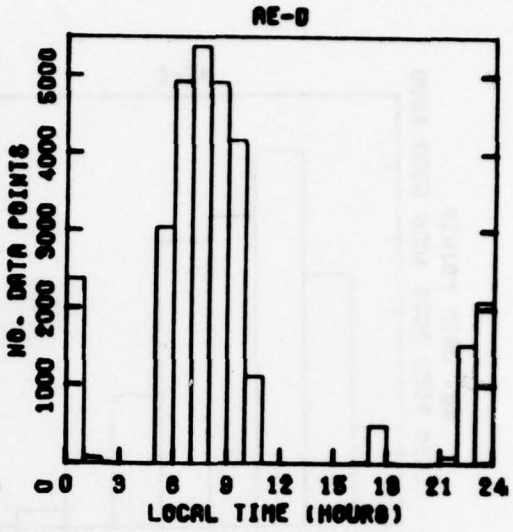

Figure 4b. Histogram of AE-D Data Distribution as a Function of Local Time

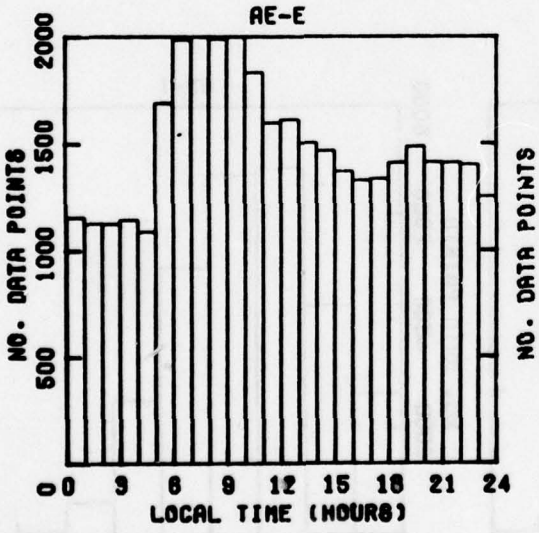

Figure 4c. Histogram of AE-E Data Distribution as a Function of Local Time

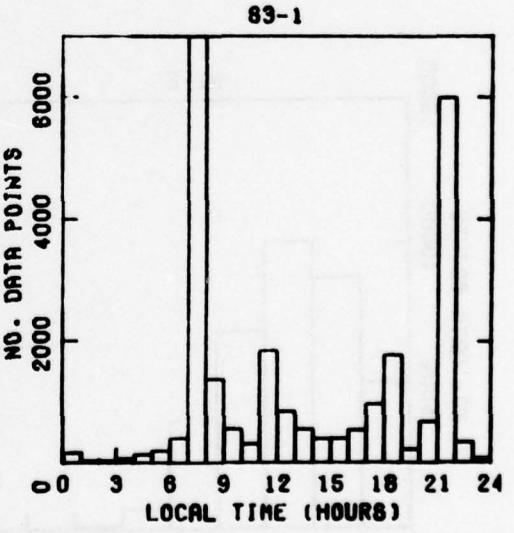

Figure 4d. Histogram of S3-1 Data Distribution as a Function of Local Time

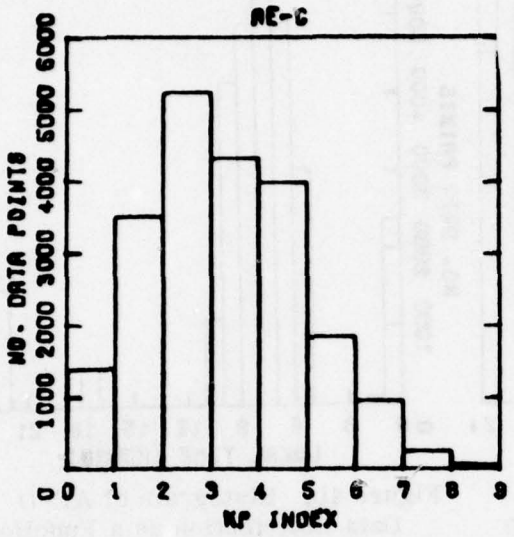

Figure 5a. Histogram of AE-C Data Distribution as a Function of Geomagnetic Activity

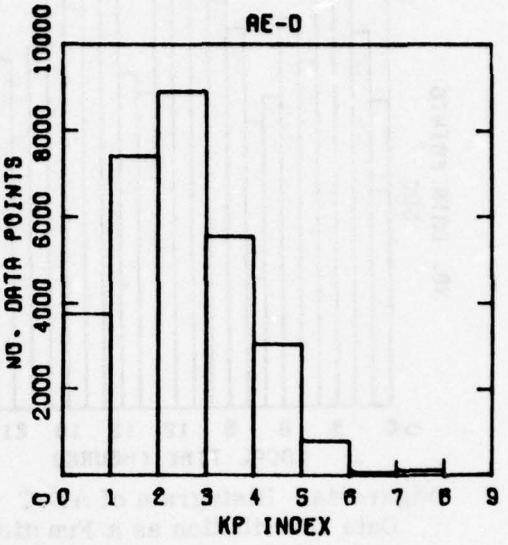

Figure 5b. Histogram of AE-D Data Distribution as a Function of Geomagnetic Activity

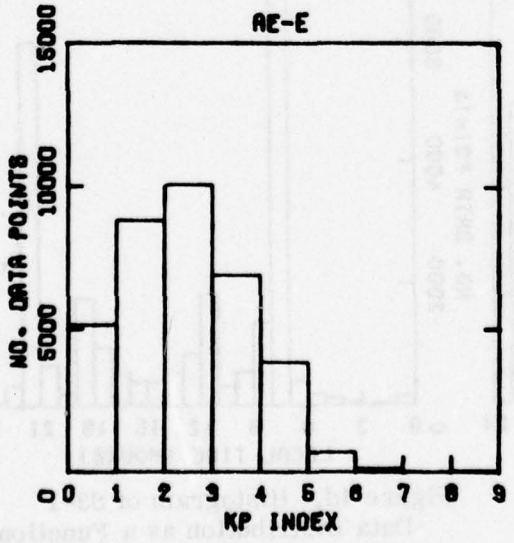

Figure 5c. Histogram of AE-E Data Distribution as a Function of Geomagnetic Activity

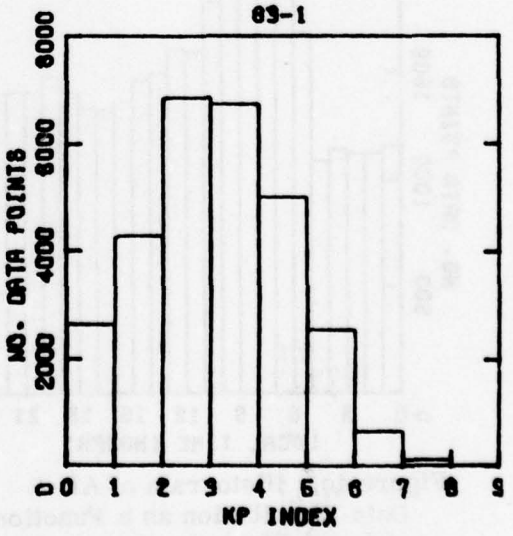

Figure 5d. Histogram of S3-1 Data Distribution as a Function of Geomagnetic Activity

is greater or equal to 4_0. In Figures 6a through 6d, distribution of data with solar flux is shown. These plots give the number of measurements during which the $F_{10.7}$ value (with a one day lag) fell within specific five solar flux unit intervals. It can be seen that the data base was obtained mainly during conditions of very low solar flux. Only about 4% of the data occur on days with $F_{10.7} > 100$. An example of the data base is given by showing results obtained at the altitude of 180 km for each satellite. Figures 7a through 7d show these density data, the latitude at which each data point was obtained, the ratio of measured density to the J71 model, and the K_p index.

2.2 Modelling

Reference (4) also compares these accelerometer density values to two commonly used atmospheric models, Jacchia 71 and MSIS. Comparisons were made as a function of altitude, latitude, geomagnetic activity and local time. Frequency distributions of the data were described in terms of the mean value and the second, third, and fourth moments about the mean.

Neither model gives a completely adequate description of the observed atmospheric variability as a function of all these atmospheric parameters. Hence we developed a multiple linear regression analysis program to attempt to generate an empirical model of atmospheric density variations in terms of latitude, longitude, local time, geomagnetic activity, solar flux, season and semi-annual effects.

In our multiple linear regression expression the dependent variable, atmospheric density, is approximated by a linear combination of a group of independent variables, that is:

$$\rho = a_0 + \sum_{i=1}^{n} a_i x_i + e_i \quad .$$

The regression technique finds the coefficients, a_i, $i=1,\ldots,n$ which minimize Σe_i^2 that is, which best describe the influence of x_i on ρ.

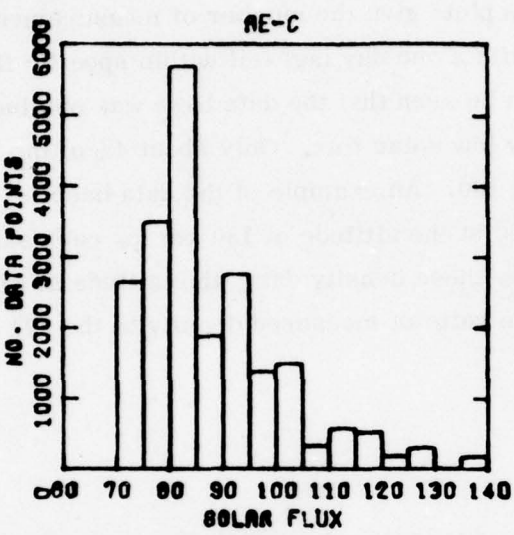

Figure 6a. Histogram of AE-C Data Distribution as a Function of Solar Flux

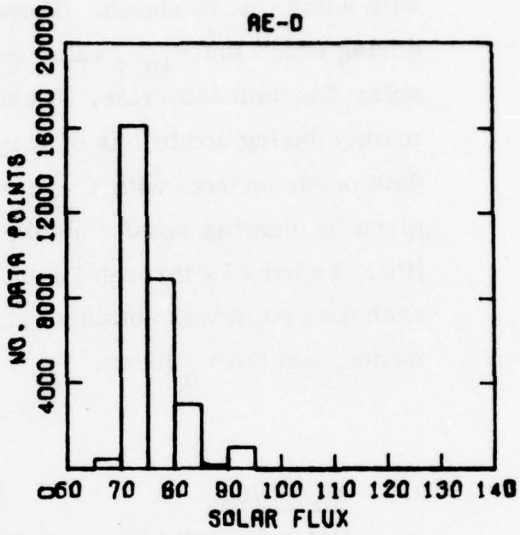

Figure 6b. Histogram of AE-D Data Distribution as a Function of Solar Flux

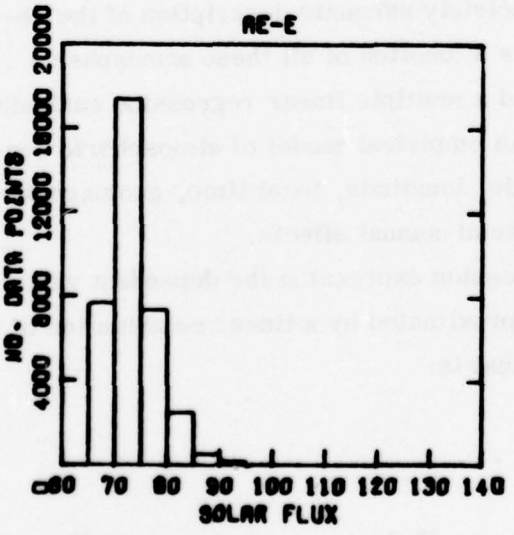

Figure 6c. Histogram of AE-E Data Distribution as a Function of Solar Flux

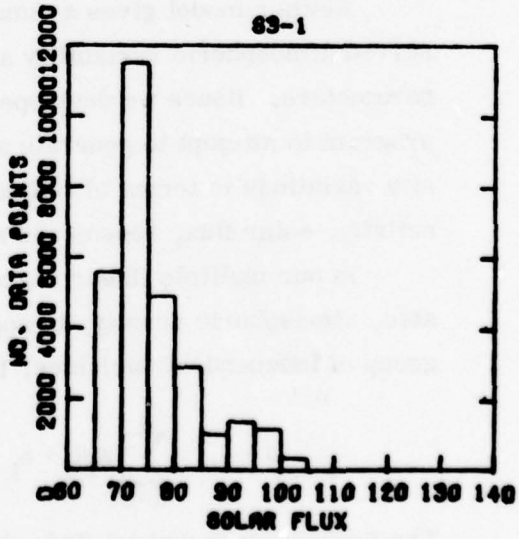

Figure 6d. Histogram of S3-1 Data Distribution as a Function of Solar Flux

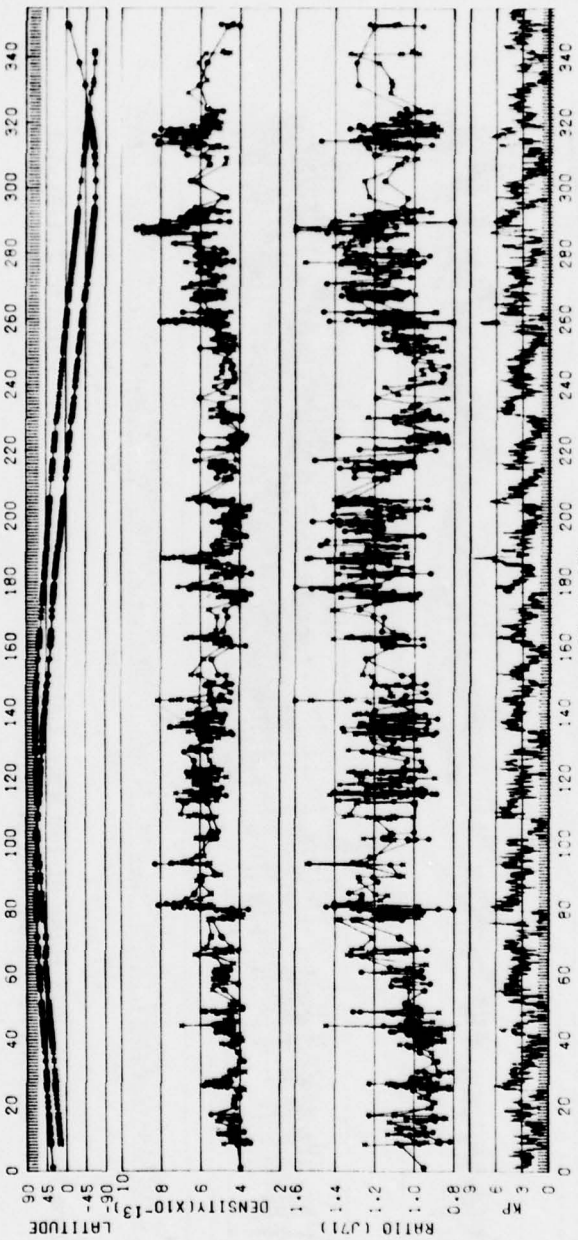

Figure 7a. AE-C Data Base at 180 km: Latitude, Density (g/cm^3) Ratio to J71 Model and Kp as a Function of Time

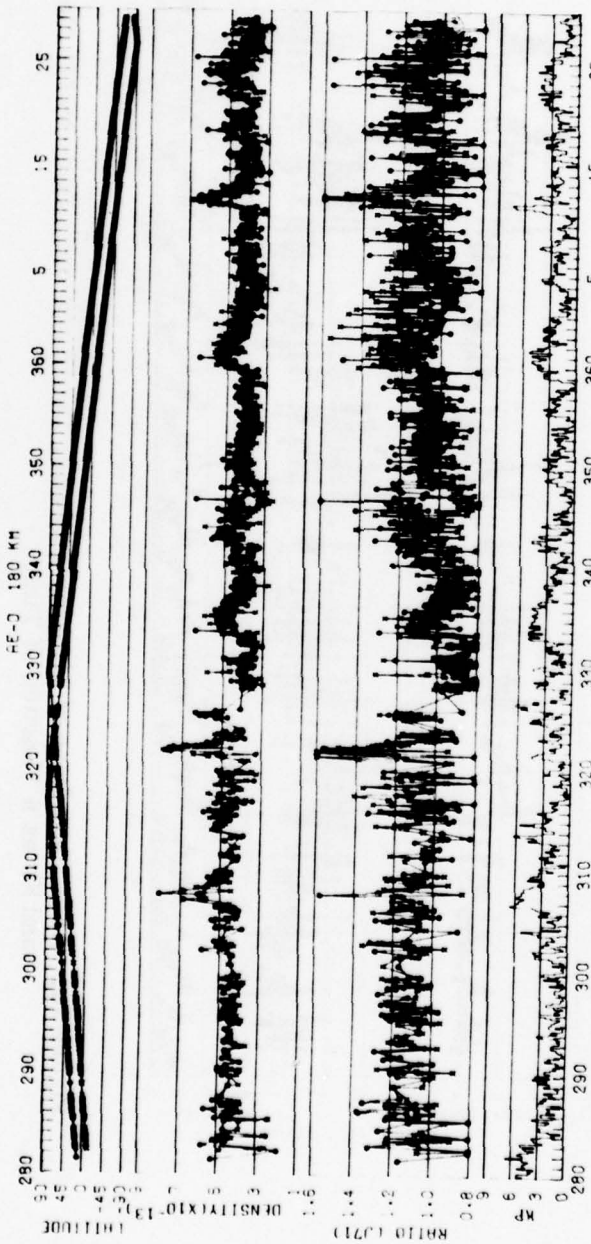

Figure 7b. AE-D Data Base at 180 km: Latitude, Density (g/cm^3) Ratio to J71 Model and Kp as a Function of Time

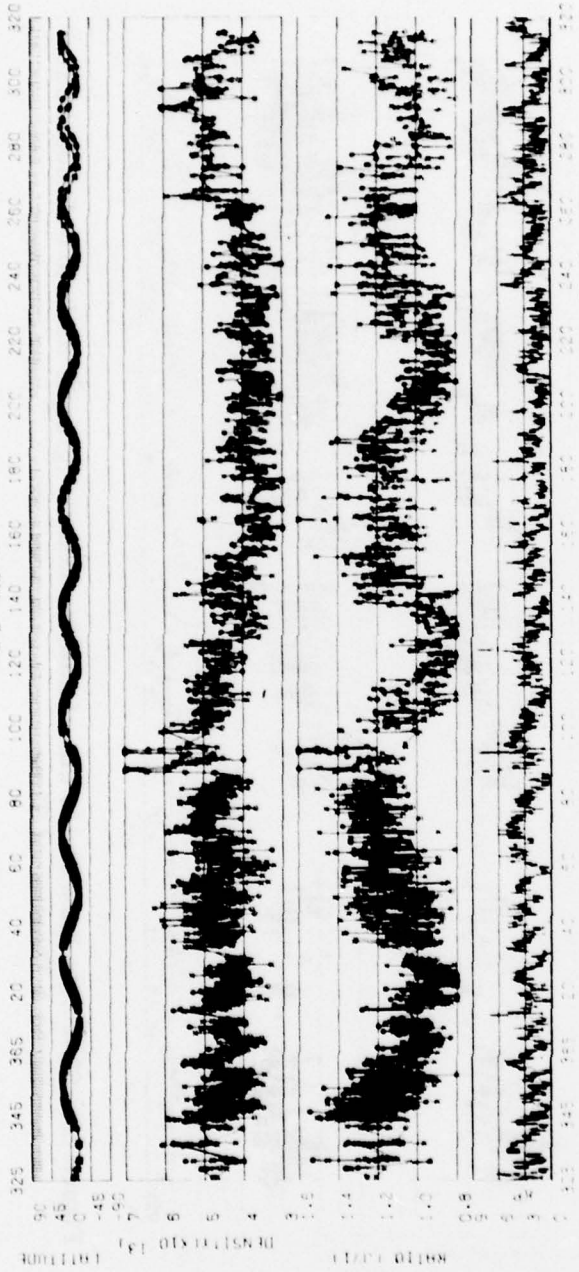

Figure 7c. AE-E Data Base at 180 km: Latitude, Density (g/cm^3) Ratio to J71 Model and Kp as a Function of Time

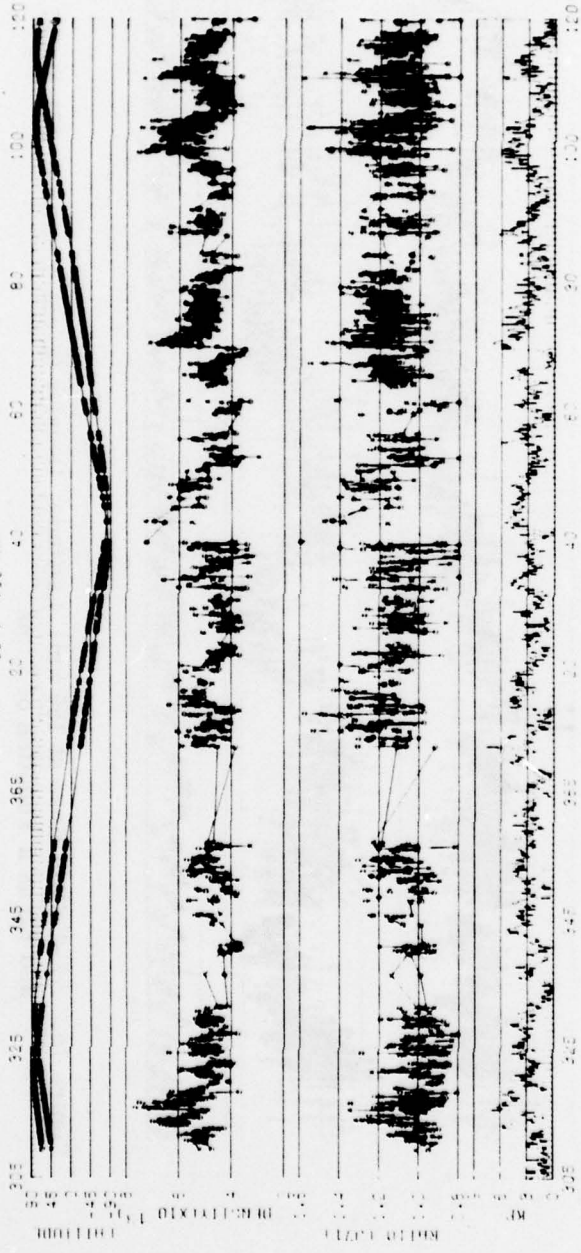

Figure 7d. S3-1 Data Base at 180 km: Latitude, Density (g/cm^3) Ratio to J71 Model and Kp as a Function of Time

The empirical model is a function of latitude, Kp, solar flux, annual and semi-annual effects, and it was run at selected satellite altitudes: 160, 180, 200, 220,and 240 km. The following table displays statistical data related to our regression analysis of AE-C data. Regression coefficients (a_i) are given at each altitude. The multiple regression coefficient (R), which is a measure of the amount of variation in the data which is described by the model, is also given.

Figure 8 displays AE-C measured density and empirical model values displayed as a function of GMT at 200 km.

The present program forms a basis for the extraction and analysis of finer density variations in the AE-C data. Additionally the program should be expanded to include the entire data base (AE-C, AE-D, AE-E and S3-1) and may be easily modified if more independent variable terms are required.

3. OTHER FUNCTIONS

3.1 Orbital Bias Determination

The accelerometer is electrostatically suspended and force rebalanced. Ground calibration requires sufficient suspension force to operate in the earth's lg field.

An important characteristic of accelerometer performance is its null bias, or output reading in the presence of no acceleration input. Instrument bias results from cross coupling of the suspension axis forces into the sensitive axis. To accurately determine atmospheric density values, the bias acceleration must be eliminated from the total sensor output. Preflight bias values are necessarily calculated using a lg suspension force. For each constrainment range, the sensor is rotated until zero output pulse rate is obtained. The sensitive axis is then rotated exactly 180°. Bias is computed from

$$\text{Bias } (\mu g) = \frac{\text{Pulse rate (pps)}}{2} \times \text{constrainment range scale factor } \frac{(\mu g)}{\text{pps}} ,$$

Table 2. Regression Analysis Results

i	F_i	a_i 160 km	a_i 180 km	a_i 200 km	a_i 220 km	a_i 240 km
0	-	1.13E-12	3.81E-13	3.80E-14	-3.56E-14	-5.03E-14
1	$Kp_{(\overline{12})}$	6.46E-14	2.56E-14	1.38E-14	7.58E-15	4.18E-15
2	Kp_6	9.70E-16	7.05E-15	3.81E-15	2.72E-15	1.72E-15
3	LAT	2.17E-15	6.39E-16	2.08E-16	1.04E-16	6.37E-17
4	$F_{10.7}$	2.71E-15	1.55E-15	1.04E-15	7.79E-16	4.58E-16
5	$\overline{F}_{10.7}$	-4.38E-15	-1.31E-15	6.51E-16	6.56E-16	6.58E-16
6	$\sin \alpha t_D$	-4.29E-14	-1.53E-14	-2.02E-15	-8.35E-16	-3.03E-16
7	$\cos \alpha t_D$	-2.56E-14	-3.16E-15	4.43E-15	5.29E-15	2.87E-15
8	$\sin 2\alpha t_D$	-1.15E-13	-4.94E-14	-2.12E-14	-1.01E-14	-4.22E-15
9	$\cos 2\alpha t_D$	-1.01E-13	-3.66E-14	-1.68E-14	-1.00E-14	-6.62E-15
10	$\sin \omega t_L$	-1.27E-14	-5.03E-15	-6.74E-15	-7.64E-15	-4.47E-15
11	$\cos \omega t_L$	-1.18E-14	-5.66E-15	-8.04E-15	-6.73E-15	-6.09E-15
12	$\sin 2\omega t_L$	-2.38E-14	2.58E-15	3.60E-15	3.31E-15	4.60E-16
13	$\cos 2\omega t_L$	8.84E-15	6.73E-15	3.06E-15	1.71E-15	3.34E-15
Number of points		1125	1143	1097	946	422
Mean density ($\bar{\rho}$)		1.30E-12	5.35E-13	2.50E-13	1.26E-13	6.80E-14
Standard deviation of $\bar{\rho}$		0.23E-12	0.96E-13	0.50E-13	0.32E-13	1.77E-14
Multiple correlation coefficient		0.78	0.79	0.79	0.73	0.75

where $\rho = a_0 + \sum_{i=1}^{13} a_i F_i$

$Kp_{(\overline{12})}$ = 12 hr average of Kp index previous to density measurement

Kp_6 = Kp 6 hrs before density measurement

LAT = geographic latitude

$F_{10.7}$ = 10.7 cm solar flux of previous day

$\overline{F}_{10.7}$ = 81 day centered average of $F_{10.7}$

$\alpha = 2\pi/365.2422$ t_D = days since 1 Jan. 1974

$\omega = 2\pi/24$ t_L = local time in hours of day

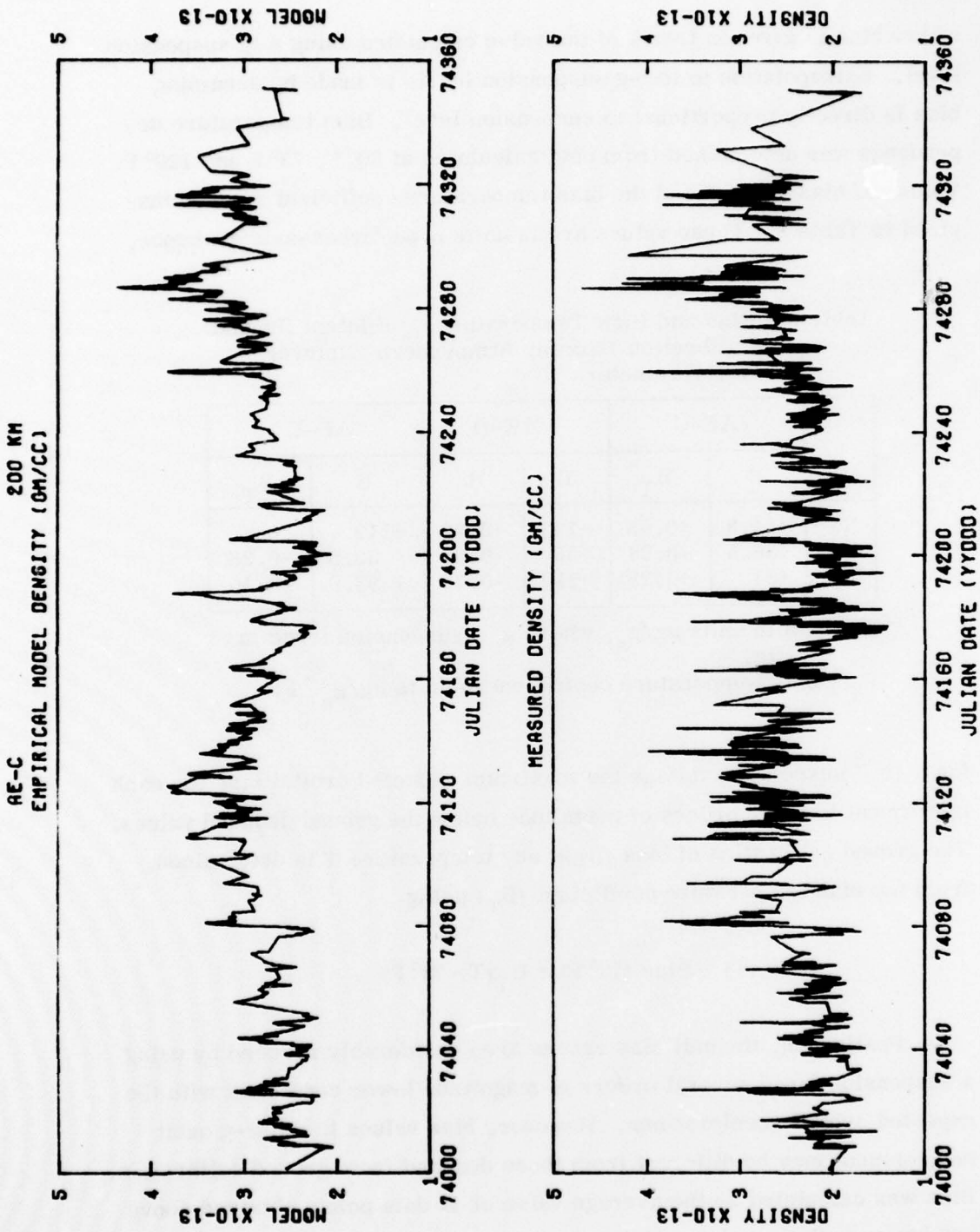

Figure 8. Measured Density and Empirical Model Results at 200 km

where bias is given in terms of the value calculated using a 1g suspension level. Extrapolation to low-g suspension levels is made by assuming bias is directly proportional to suspension level. Bias temperature dependence was determined from data calculated at 30° F, 73° F and 120° F. Values of bias at 73° F and the bias temperature coefficient are summarized in Table 3. These values are in units of μg/cross-axis g; hence,

Table 3. Bias and Bias Temperature Coefficient Ground Calibration Data for Atmosphere Explorer Accelerometers

	AE-C		AE-D		AE-E	
	B	B_T	B	B_T	B	B_T
XY	+54.3	+0.05	+103	+0.20	+112	0
YX	+36.5	-0.24	+35	-0.99	+ 52.5	-0.26
ZZ	+81	+0.28	+110	-0.73	+ 93.8	-0.46

B = bias in units $\mu g/g_s$, where g_s = suspension force in g units.

B_T = bias temperature coefficient in units $\mu g/g_s$ °F.

for a 10^{-3} suspension voltage the maximum expected orbital bias for each instrument is three orders of magnitude below the ground deduced values. The ground calibration of bias (B) at any temperature T is determined from the bias temperature coefficient (B_T) using

$$\text{Bias (T)} = \text{Bias (73° F)} + B_T(T - 73° F) \ .$$

Postlaunch, the null bias errors are considerably reduced by using a suspension force several orders of magnitude lower consistent with the expected orbital accelerations. However, bias values in a low-g orbit environment may be different from those deduced from ground calibration. Bias was calculated as the average value of 48 data points obtained above 360 km on both the upleg and downleg portion of elliptical orbits. Data are presented for the XY instrument on AE-C, and the YX instrument on AE-D and AE-E.

Table 4 summarizes the orbital data from the three instruments studied. This table gives bias values at 73° and the standard deviations (in parenthesis), the bias temperature coefficients, and the factor by which orbital bias was reduced as a result of lowering the sensor suspension voltage to 10^{-3} g.

Table 4. Orbital Bias and Bias Temperature Coefficient Results

	AE-C	AE-D	AE-E
Bias (Standard Deviation)	1.270 μg (0.133 μg)	-1.130 μg (0.268 μg)	-4.632 μg (0.054 μg)
Bias Temperature Coefficient	-0.0026 μg/° F	-0.0335 μg/° F	-0.0205 μg/° F
Reduction Factor from lg value	42.7	31.0	11.3
No. data points	400	300	334

The long term stability of the orbital bias data and its temperature dependence, indicate that the above determined values can be used for reduction of density data when routine bias measurements are not possible. These results show that bias must be determined in orbit rather than from ground calibration for accurate drag measurements in despun orbits.

For a more complete description of AE accelerometer orbital bias determination see Reference (5).

3.2 Correlative Measurements

Density data base development was previously described in Section 1.3. In order to correlate long term density variations with other experiments on AE, we were required to create similar data bases from two AE experiments – Open-Source Neutral-Mass Spectrometer (OSS) and Neutral-Atmosphere Composition Experiment (NACE). This was carried out utilizing the same methods as described in Section 1.3 using the OSS and NACE unified abstract history files on the AE computer.

Composition data were calculated at 10-km intervals from 140 km to 200 km for AE-C utilizing interpolation techniques. These data were stored in data files on the AE computer and later shipped to AFGL for use on the AFGL computer system.

At AFGL OSS composition data were merged with MESA density data, total mass density values were calculated and comparisons to MESA values were made. Figures 9 to 11 illustrate some of the comparisons which were made. Further such studies are contemplated.

3.3 Circular Orbit Processing

The objectives of the AE missions was to study phenomena in the atmosphere at altitudes above 120 km. This was to be accomplished in two orbital phases: elliptic orbit and circular orbit. After the initial elliptic orbit phase was completed, AE-C and AE-E were circularized for the second phase of their mission.

For circular orbit spinning data our processing techniques to calculate density (Reference (2)) were for the most part unchanged. For despun circular orbits, since instrument bias values are required and the satellite altitude was below the "non-drag regions" used in the elliptic orbit phase, an alternate method was required to determine bias values. We utilized the techniques described in Section 3.1 above and Reference (5) to calculate bias temperature coefficients for each satellite. Circular orbit temperature data was then used to calculate instrument bias values, and filtering techniques were used to determine density values. Circular orbit density data are being calculated in a production environment and stored in the AE unified abstract files.

One method of analyzing circular orbit data is to normalize calculated density values to any altitude utilizing model atmosphere theory. This is done by:

$$\text{normalized density} = \frac{\text{measured density} \times \text{model density (at the normalized altitude)}}{\text{model density}}$$

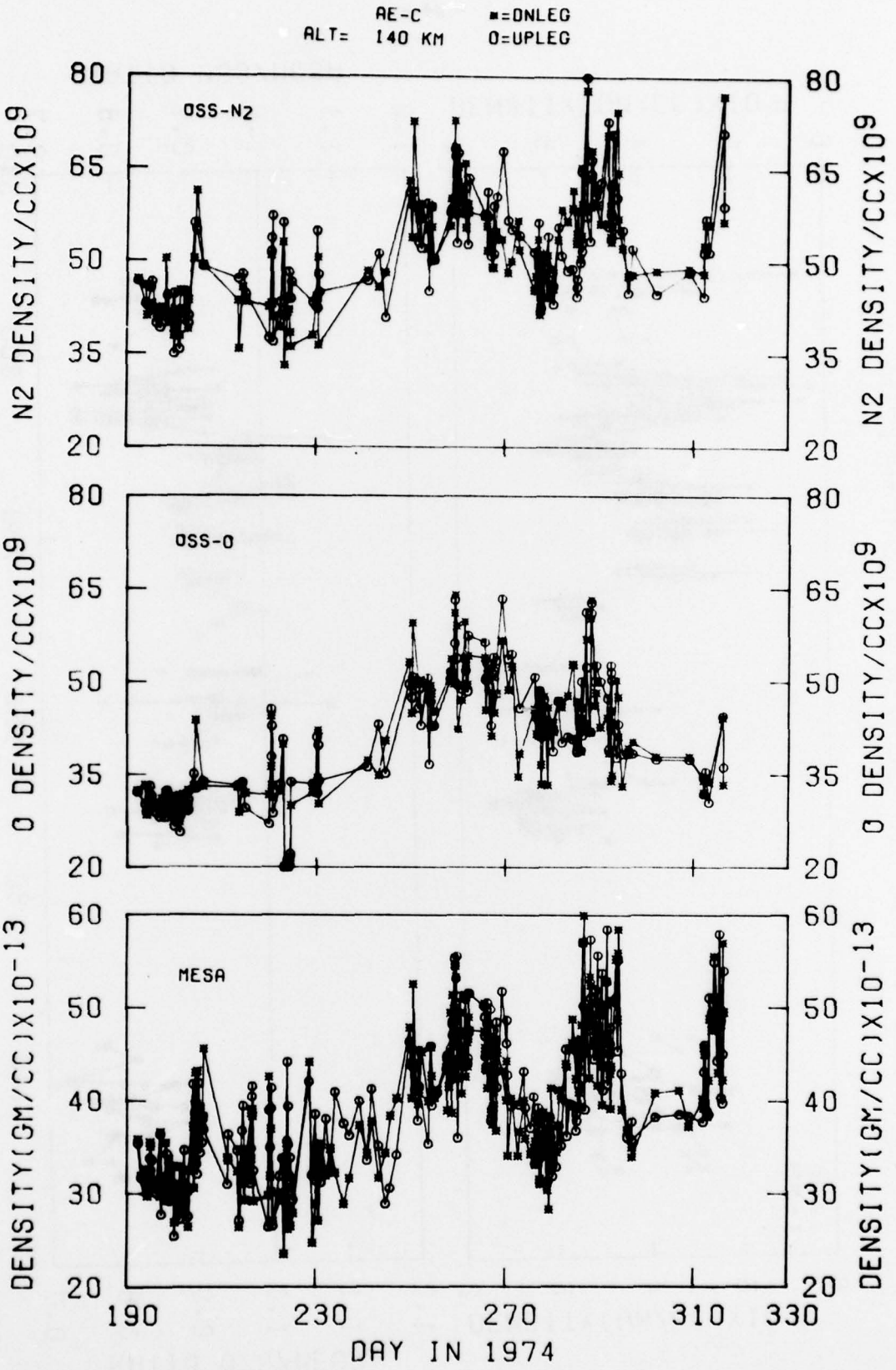

Figure 9. AE-C MESA Density, OSS-O and N2 Density Results at 140 km

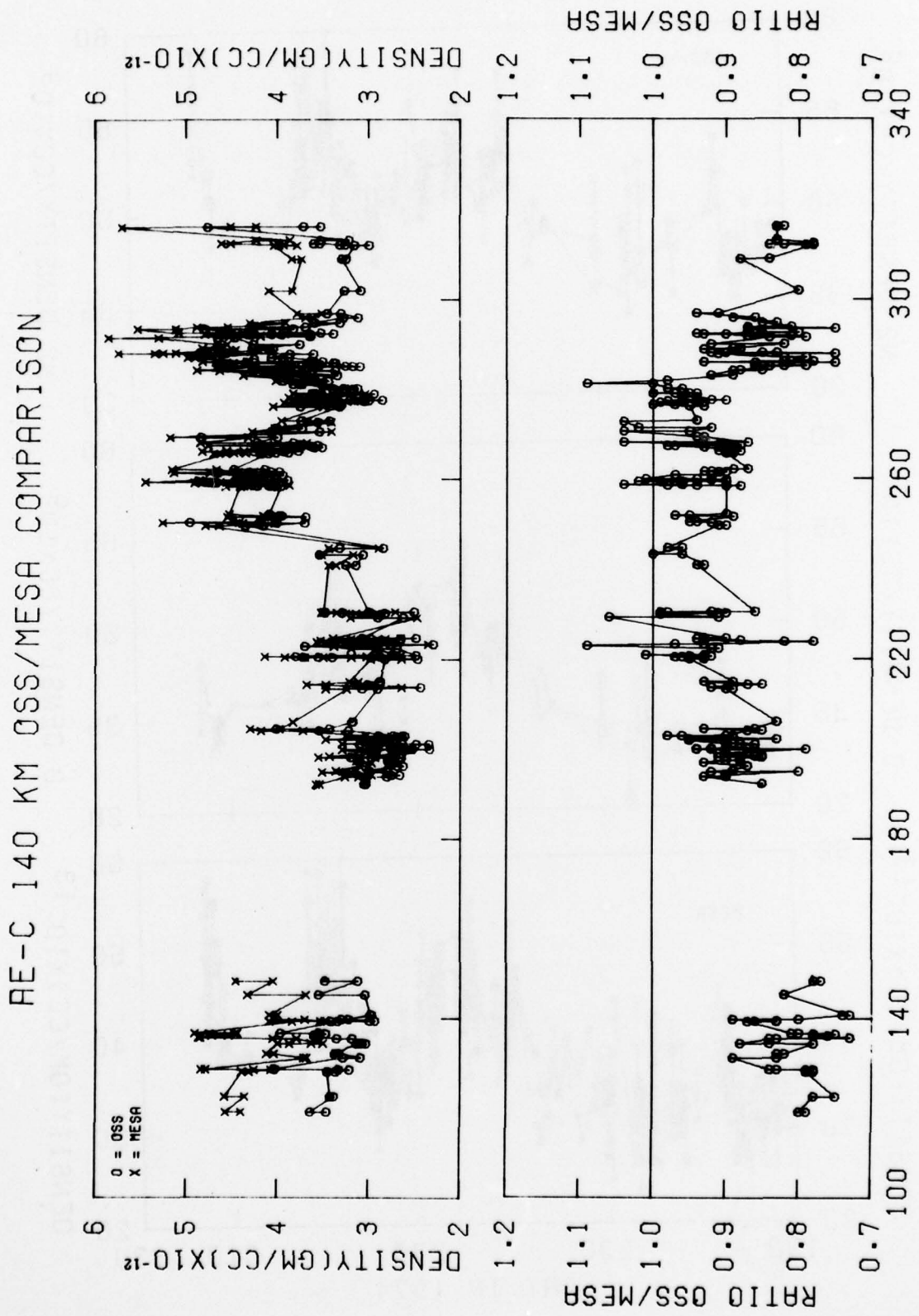

Figure 10. AE-C OSS/MESA Density Comparison at 140 km

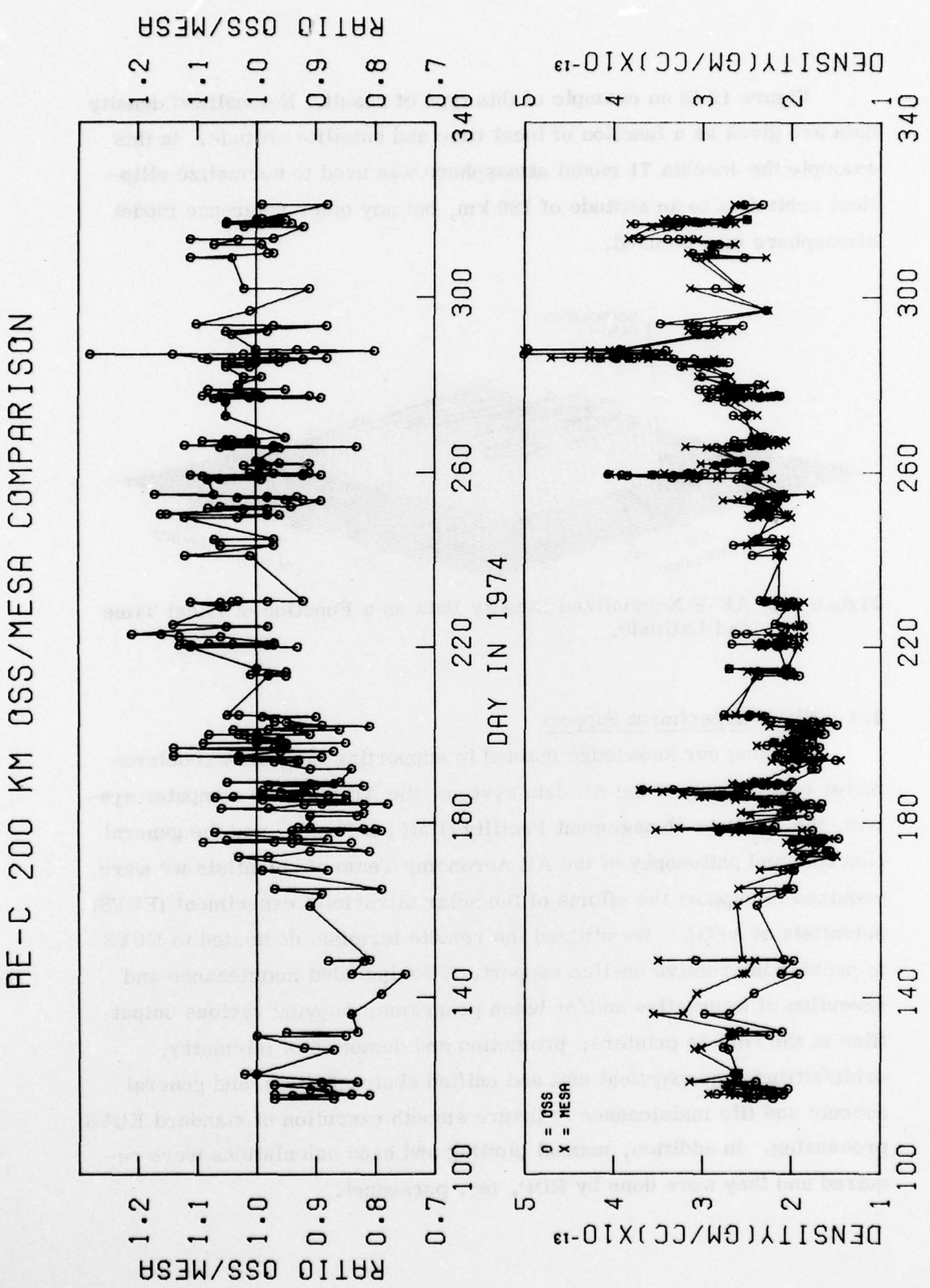

Figure 11. AE-C OSS/MESA Density Comparison at 200 km

Figure 12 is an example of this type of result. Normalized density data are given as a function of local time and satellite altitude. In this example the Jacchia 71 model atmosphere was used to normalize elliptical orbit data to an altitude of 180 km, but any other reference model atmosphere may be used.

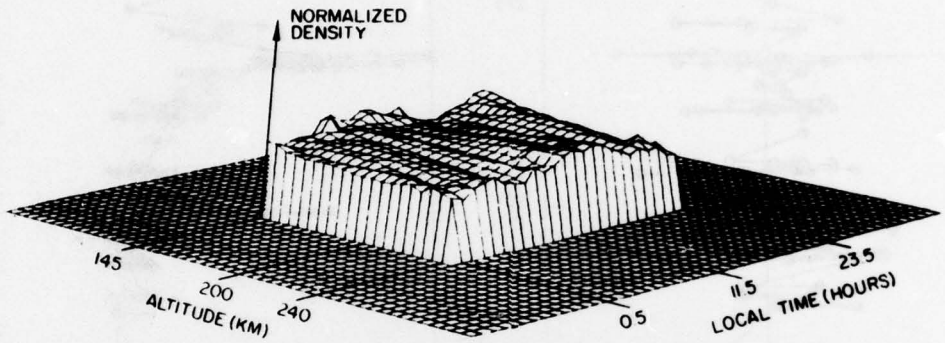

Figure 12. AE-E Normalized Density Data as a Function of Local Time and Latitude.

3.4 EUVS Experiment Support

Utilizing our knowledge (gained in supporting the MESA accelerometer experiment) of the AE data system, the AE Sigma-9 computer system, the AE Data Management Facility (DMF) software, and the general concepts and philosophy of the AE Aeronomy Team of scientists we were required to support the efforts of the solar ultraviolet experiment (EUVS) scientists at AFGL. We utilized the remote terminal dedicated to EUVS to provide interactive on-line support. This included maintenance and execution of interactive and/or batch programs; copying various output files to the remote printers; promotion and demotion of telemetry, orbit/attitude, geophysical unit and unified abstract files; and general account and file maintenance to insure smooth execution of standard EUVS processing. In addition, manual plotting and hand calculations were required and they were done by RDP, Inc. personnel.

4. CONCLUSIONS

An extensive data base has been developed utilizing accelerometer measurements obtained with four low altitude satellites. In addition to density values the data base incorporates appropriate satellite orbital information, solar and geophysical parameters and atmospheric model values. It is anticipated that this data base will be useful for correlative studies of aeronomical problems requiring knowledge of the neutral atmosphere, as well as an improved model of the lower thermosphere.

5. ACKNOWLEDGEMENTS

We wish to acknowledge the support of Frank A. Marcos, AFGL (LKB), Contract Monitor, for his evaluation and recommendations in the application of these efforts to the AE data.

Implementation of mathematical analyses and development of computer plotting programs were provided by RDP, Inc. staff members, Dr. C. John McCann and Shirley J. Cieszka, respectively.

6. REFERENCES

[1] Fioretti, R.W., Ed., (1976), Atmosphere Explorer MESA Accelerometer Data Processing System, AFGL-TR-76-0137, AFGL, Massachusetts.

[2] Noonan, J.P., Fioretti, R.W., and Hass, B., (1975), Digital Filtering Analysis Applied to the Atmosphere Exporer-C Satellite MESA Accelerometer Data, AFCRL-75-0293, AFCRL, Massachusetts.

[3] Champion, K.S.W., and Marcos, F.A., (1973), The Triaxial Accelerometer System on Atmosphere Explorer, Radio Science, Vol. 8.

[4] Marcos, F.A., McInerney, R.E. and Fioretti, R.W., (1978), Variability of the Lower Thermosphere Determined from Satellite Accelerometer Data, AFGL-TR-78-0134, AFGL, Massachusetts.

[5] Marcos, F.A. and Fioretti, R.W., (1977), Orbital Bias Determination for Accelerometers on Atmosphere Explorer Satellites, AFGL-TR-77-0147, AFGL, Massachusetts.